

Modeling growth, lipid accumulation and lipid turnover in submerged batch cultures of *Umbelopsis isabellina*

Petra Meeuwse · Payman Akbari ·
Johannes Tramper · Arjen Rinzema

Received: 15 June 2011 / Accepted: 15 September 2011
© The Author(s) 2011. This article is published with open access at Springerlink.com

Abstract The production of lipids by oleaginous yeast and fungi becomes more important because these lipids can be used for biodiesel production. To understand the process of lipid production better, we developed a model for growth, lipid production and lipid turnover in submerged batch fermentation. This model describes three subsequent phases: exponential growth when both a C-source and an N-source are available, carbohydrate and lipid production when the N-source is exhausted and turnover of accumulated lipids when the C-source is exhausted. The model was validated with submerged batch cultures of the fungus *Umbelopsis isabellina* (formerly known as *Mortierella isabellina*) with two different initial C/N-ratios. Comparison with chemostat cultures with the same strain showed a significant difference in lipid production: in batch cultures, the initial specific lipid production rate was almost four times higher than in chemostat cultures but it decreased exponentially in time, while the maximum specific lipid production rate in chemostat cultures was independent of residence time. This indicates that different mechanisms for lipid production are active in batch and chemostat cultures. The model could also describe data for submerged batch cultures from literature well.

Keywords Submerged batch culture ·
Umbelopsis isabellina · Oleaginous fungi ·
Kinetic model · Biodiesel

List of symbols

C_N	N-source concentration (Nmol m ⁻³)
C_L	Lipid concentration (Cmol m ⁻³)
C_P	Carbohydrate concentration (Cmol m ⁻³)
C_S	C-source concentration (Cmol m ⁻³)
C_X	Basic biomass concentration (Cmol m ⁻³)
C_{Xmax}	Maximum basic biomass concentration (Cmol m ⁻³)
f_{L0}	Minimum fraction of lipids in total biomass [Cmol lipids (Cmol total biomass) ⁻¹]
f_{Pmax}	Maximum fraction of carbohydrates in the cells [Cmol carbohydrates (Cmol basic biomass) ⁻¹]
k_d	Lipid production rate degradation constant (h ⁻¹)
m_L	Maintenance coefficient on lipids (Cmol Cmol ⁻¹ h ⁻¹)
m_S	Maintenance coefficient on C-source (Cmol Cmol ⁻¹ h ⁻¹)
r_C	CO ₂ -production rate (Cmol m ⁻³ h ⁻¹)
r_L	Lipid production rate (Cmol m ⁻³ h ⁻¹)
r_N	N-source production rate (Nmol m ⁻³ h ⁻¹)
r_O	Oxygen production rate (mol m ⁻³ h ⁻¹)
r_P	Carbohydrate production rate (Cmol m ⁻³ h ⁻¹)
r_S	C-source production rate (Cmol m ⁻³ h ⁻¹)
r_W	Water production rate (mol m ⁻³ h ⁻¹)
r_X	Basic biomass production rate (Cmol m ⁻³ h ⁻¹)
t	Time (h)
t_{12}	Time point of transition from growth phase to lipid production phase (h)
t_{2ab}	Time point where the maximum carbohydrate fraction is reached (h)
t_{23}	Time point of transition from lipid production phase to lipid turnover phase (h)
q_L	Specific lipid production rate (Cmol Cmol ⁻¹ h ⁻¹)
q_{Lmax}	Maximum specific lipid production rate (Cmol Cmol ⁻¹ h ⁻¹)

P. Meeuwse · P. Akbari · J. Tramper · A. Rinzema (✉)
Bioprocess Engineering, Wageningen University,
P.O. Box 8129, 6700 EV Wageningen, The Netherlands
e-mail: Arjen.rinzema@wur.nl

q_P	Specific carbohydrate production rate (Cmol Cmol ⁻¹ h ⁻¹)
Y_{LS}	Yield of lipids on C-source (Cmol Cmol ⁻¹)
Y_{PS}	Yield of carbohydrates on C-source (Cmol Cmol ⁻¹)
Y_{XN}	Yield of lipid-free biomass on nitrogen source (Cmol Nmol ⁻¹)
Y_{XS}	Yield of lipid-free biomass on C-source (Cmol Cmol ⁻¹)
γ_O	Degree of reduction of oxygen = -4 mol^{-1}
γ_X	Degree of reduction of lipid-free biomass = 4.16 Cmol^{-1}
γ_L	Degree of reduction of lipids = 5.73 Cmol^{-1}
γ_S	Degree of reduction of C-source = 4 Cmol^{-1} (glucose)
γ_P	Degree of reduction of carbohydrates = 4 Cmol^{-1}
μ_{\max}	Maximum specific growth rate (h ⁻¹)

Introduction

Research on lipid accumulation in oleaginous yeast and fungi has long been focused on the production of polyunsaturated fatty acids such as arachidonic acid and γ -linolenic acid [1]. More recently, production of lipids as a feedstock for biodiesel also gets attention [2–4]. Microbial lipids for biodiesel production are a bulk product and therefore have to be produced at low cost. The method used for PUFA production, i.e. cultivation of oleaginous yeast or fungi in submerged cultures on a substrate such as glucose, is expensive because bioreactor costs and substrate costs are high. The development of a new and cheaper process requires knowledge about the mechanisms involved and the kinetics. A mathematical model can help to structure this knowledge and can be used as a tool to improve the production. This paper presents a model for the bioconversion kinetics in submerged batch cultures of a lipid-accumulating fungus.

Several mathematical models for lipid production in submerged batch culture are already available in the literature. Granger et al. [5] and Sattur and Karanth [6] developed stoichiometric models for prediction of the final lipid concentration in a batch culture from initial substrate concentrations. These models do not take reaction kinetics into account and are therefore not suitable to describe cultures in time. Sattur and Karanth [7, 8] developed a kinetic model for growth and lipid accumulation based on the logistic law and the Luedeking–Piret model. Their models do not describe depletion of the N-source, which is an important factor for lipid production [9]. Several models

of Aggelis and co-workers [10–12] describe growth and lipid production on various lipid-based substrates, but do not take depletion of the N-source into account. Glatz et al. [13] and Economou et al. [14] modeled growth and lipid accumulation using Monod kinetics and a mathematical function that gives a gradual transition from growth to lipid accumulation as the N-source gets depleted. Economou et al. [14] also included substrate inhibition and lipid turnover; substrate inhibition was observed but lipid turnover was not observed.

Our experiments show that there are two aspects of a submerged batch culture with oleaginous fungi that were not properly described in the aforementioned models. First, we observed a decrease in the lipid production rate in batch cultures that is not caused by the decline in C-source concentration; this was reported before [15] but not described in previous models [13, 14]. Second, lipid turnover was in previous models [10–12, 14] associated with growth, which is not in agreement with our results. Instead, we observed lipid turnover for maintenance.

We developed a new model for lipid accumulation in batch cultures including the two afore mentioned aspects, based on our previously developed model for lipid production in chemostat cultures [16, 17]. The model describes the experimental data present in this paper as well as data from literature well, which shows that it is more generally applicable.

Model

Figure 1 shows a simplified scheme of the metabolism of an oleaginous organism [16]. The organism uses a C-source (S), an N-source (N) and oxygen (O) to produce cell material (X), lipids (L), carbohydrates (P), carbon dioxide (C) and water (W). For calculations, the biomass is divided into lipids, carbohydrates and lipid-free, carbohydrate-free biomass; the latter is referred to as basic biomass. The composition of basic biomass [CH_{1.77}O_{0.55}N_{0.17}, MW = 28.7 g Cmol⁻¹ including 13% (w/w) ash] is based on the average composition of *Umbelopsis isabellina* during exponential growth in the experiments, and the composition of the lipids (CH_{1.95}O_{0.11}, MW = 15.7 g Cmol⁻¹) is based on the average fatty acid composition of the accumulated triacylglycerol in *U. isabellina* during the experiments. Concentrations of all components that contain carbon are expressed in Cmoles; O₂ and NH₃ are expressed in moles and Nmoles, respectively.

The model is based on Fig. 1 and several assumptions:

- Oxygen is not limiting.

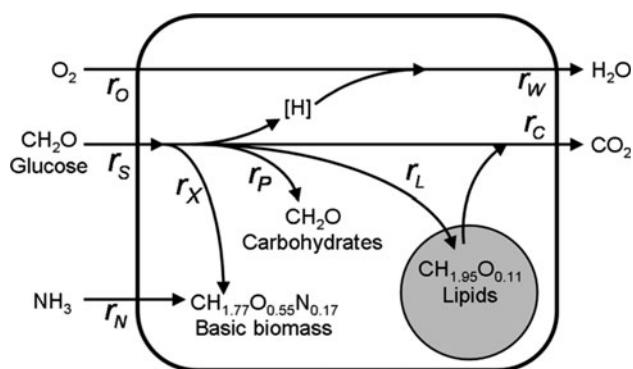


Fig. 1 Schematic overview of carbon and nitrogen metabolism of the oleaginous fungus *U. isabellina*. The substrates oxygen (r_O), glucose (r_S) and ammonium (r_N) are consumed to produce basic biomass (r_X), carbohydrates (r_P), lipids (r_L), water (r_W) and CO_2 (r_C). The composition of basic biomass and lipids are based on experimental results

- The N-source in the substrate is exhausted before the C-source.
- A batch culture consists of three subsequent phases: (1) As long as both N-source and C-source are available, the fungus grows and synthesizes only functional lipids (for membranes, etc.). (2) After the N-source is depleted, the fungus accumulates lipids and storage carbohydrates in its cells until the C-source is depleted. (3) After the substrate C-source is depleted, the fungus uses the lipids stored in its cells for maintenance; stored carbohydrates are shown not to be consumed.
- The C-source is a monomer and the N-source an inorganic compound; no hydrolysis of polymers is needed.
- The initial C-source and N-source concentrations are not inhibitory.
- After depletion of the N-source, the cells accumulate lipids and another storage compound, which we assume to be carbohydrates (CH_2O). Glycogen and trehalose are important storage products in many fungi [18, 19] and carbohydrate storage has been demonstrated in oleaginous yeasts [20, 21]. We assume that all carbon-containing storage components that cannot be extracted with chloroform are carbohydrates.
- No other carbon or nitrogen-containing products are produced besides basic biomass, carbohydrates, lipids and CO_2 .
- The C-source and N-source concentrations do not affect the conversion rates of these components (zero-order kinetics with respect to reactants).

We will now discuss the three different phases in a batch process and further assumptions made for each phase. All balances used are differential equations, but we only show the integrated forms.

Phase 1: Exponential growth phase

During the exponential growth phase, basic biomass with a basal fraction of functional lipids is formed and C-source and N-source are consumed. We assume that none of the substrates is limiting for growth in this phase. Therefore, the cells will grow exponentially with their maximum specific growth rate and the basic biomass concentration is given by:

$$C_X(t) = C_X(0)e^{\mu_{\max}t}. \quad (1)$$

The cells have a constant basal lipid fraction (f_{L0}). Therefore, the lipid concentration is proportional to the basic biomass concentration:

$$C_L(t) = \frac{f_{L0}}{1 - f_{L0}} C_X(t). \quad (2)$$

Carbohydrates formed during phase 1 are included in the basic biomass and not calculated separately ($C_P = 0$).

We assume a linear relation between the rates of N-source conversion and basic biomass production and use Pirt's law for the conversion rate of the C-source. This gives for the concentrations of N-source and C-source:

$$C_N(t) = C_N(0) - \frac{C_X(t) - C_X(0)}{Y_{XN}} \quad (3)$$

$$C_S(t) = C_S(0) - \left(\frac{\mu_{\max}}{Y_{XS}} + \frac{f_{L0}}{1 - f_{L0}} \frac{\mu_{\max}}{Y_{LS}} + m_S \right) \frac{C_X(t) - C_X(0)}{\mu_{\max}}. \quad (4)$$

The CO_2 -production rate is found from the C-balance:

$$r_C(t) = \left(\left(\frac{1}{Y_{XS}} - 1 + \frac{f_{L0}}{1 - f_{L0}} \left(\frac{1}{Y_{LS}} - 1 \right) \right) \mu_{\max} + m_S \right) C_X(t). \quad (5)$$

An electron balance gives the O_2 -consumption rate:

$$-r_O(t) = \frac{1}{-\gamma_O} \left(\left(\gamma_X - \frac{\gamma_S}{Y_{XS}} + \frac{f_{L0}}{1 - f_{L0}} \left(\gamma_L - \frac{\gamma_S}{Y_{LS}} \right) \right) \mu_{\max} - \gamma_S m_S \right) C_X(t). \quad (6)$$

The exponential growth phase ends at $t = t_{12}$ when the N-source is depleted (derived from Eqs. 1, 3):

$$t_{12} = \frac{1}{\mu_{\max}} \ln \left(\frac{Y_{XN} C_N(0)}{C_X(0)} + 1 \right). \quad (7)$$

The basic biomass has then reached its maximum value:

$$C_{X\max} = C_X(0) + Y_{XN} C_N(0). \quad (8)$$

Phase 2: Lipid accumulation phase

After the N-source is depleted, the cells no longer grow but do continue to use the C-source for maintenance, carbohydrate production and lipid production. The experimental results show that the specific lipid production rate decreases exponentially in this phase. This gives for the lipid concentration:

$$C_L(t) = \left(\frac{f_{L0}}{1-f_{L0}} + \frac{q_{Lmax}}{k_d} \left(1 - e^{-k_d(t-t_{12})} \right) \right) C_{Xmax}. \quad (9)$$

At the beginning of phase 2, we assume accumulation of carbohydrates at a constant rate, until the maximum carbohydrate fraction in the cells is reached:

$$C_P(t) = q_P C_{Xmax} (t - t_{12}) \leq f_{Pmax} C_{Xmax}. \quad (10)$$

This means that phase 2 can be divided in two parts: part 2a in which carbohydrates are produced, and part 2b in which the cells have a constant maximum carbohydrate fraction. The time at which the maximum carbohydrate fraction is reached, t_{2ab} , is equal to:

$$t_{2ab} = t_{12} + \frac{f_{Pmax}}{q_P}. \quad (11)$$

We assume that the specific carbohydrate production rate (q_P) is limited by the maximum specific C-source uptake rate of the cells, which corresponds to the specific rate during exponential growth:

$$\begin{aligned} \frac{\mu_{max}}{Y_{XS}} + \frac{f_{L0}}{1-f_{L0}} \frac{\mu_{max}}{Y_{LS}} + m_S &= \frac{q_L}{Y_{LS}} + \frac{q_P}{Y_{PS}} + m_S \rightarrow \\ q_P &= Y_{PS} \left(\frac{\mu_{max}}{Y_{XS}} + \frac{f_{L0}}{1-f_{L0}} \frac{\mu_{max}}{Y_{LS}} - \frac{q_L}{Y_{LS}} \right). \end{aligned} \quad (12)$$

The C-source concentration in phases 2a and 2b is then obtained from Pirt's law and a mass balance for the C-source:

$$\begin{cases} t < t_{2ab} : C_S(t) = C_S(t_{12}) - \left(\frac{q_{Lmax}}{Y_{LS}k_d} \left(1 - e^{-k_d(t-t_{12})} \right) + \left(\frac{q_P}{Y_{PS}} + m_S \right) (t - t_{12}) \right) C_{Xmax} \\ t \geq t_{2ab} : C_S(t) = C_S(t_{2ab}) - \left(\frac{q_{Lmax}}{Y_{LS}k_d} \left(e^{-k_d(t_{2ab}-t_{12})} - e^{-k_d(t-t_{12})} \right) + m_S (t - t_{2ab}) \right) C_{Xmax} \end{cases} \quad (13)$$

The respiration rates are again obtained from the C-balance and the electron balance, respectively:

$$\begin{aligned} r_C(t) &= \left(\left(\frac{1}{Y_{LS}} - 1 \right) q_{Lmax} e^{-k_d(t-t_{12})} \right. \\ &\quad \left. + \left(\frac{1}{Y_{PS}} - 1 \right) q_P(t) + m_S \right) C_{Xmax} \end{aligned} \quad (14)$$

$$\begin{aligned} -r_O(t) &= \frac{1}{-\gamma_O} \left(\left(\gamma_L - \frac{\gamma_S}{Y_{LS}} \right) q_{Lmax} e^{-k_d(t-t_{12})} \right. \\ &\quad \left. + \left(\gamma_P - \frac{\gamma_S}{Y_{PS}} \right) q_P(t) - \gamma_S m_S \right) C_{Xmax}. \end{aligned} \quad (15)$$

Phase 2 ends when the C-source is depleted. Equation 13 can be used to find the time of transition to phase 3, t_{23} , by iteration.

Phase 3: Lipid turnover phase

When the C-source in the medium is exhausted, the cells use the accumulated lipids for maintenance. The mass balance for lipids gives:

$$C_L(t) = C_L(t_{23}) - m_L C_{Xmax} (t - t_{23}). \quad (16)$$

Lipid combustion generates 1.4 times more ATP per Cmol than glucose combustion, hence:

$$m_L = m_S / 1.4. \quad (17)$$

In contrast to our expectations, the accumulated carbohydrates were not consumed in our experiments, and we have therefore not included carbohydrate turnover in the model.

The respiration rates in phase 3 are:

$$r_C(t) = m_L C_{Xmax} \quad (18)$$

$$-r_O(t) = \frac{\gamma_L}{-\gamma_O} m_L C_{Xmax}. \quad (19)$$

Materials and methods

Medium

Liquid medium for all cultures contained per liter 0.5 g KCl, 0.5 g MgSO₄·7H₂O, 1.5 g Na₂HPO₄·2H₂O, 1 mL

trace metal solution as described by Vishniac and Santer [22], glucose as C-source and (NH₄)₂SO₄ as N-source. Pre-culture medium contained 100 mM glucose and 100 mM NH₄⁺. Culture medium contained 100 mM glucose and 20 mM NH₄⁺, resulting in an initial C/N-ratio of 30 Cmol Nmol⁻¹. The pH of all media was adjusted to 6.0 by adding H₂SO₄. The glucose was autoclaved separately.

To the fermentation medium, 1 mL of antifoam [Polypropylene glycol (Sigma), 50% v/v in ethanol] was added per liter.

Pre-culture

The pre-culture was carried out in 250-mL shake flasks with 100 mL pre-culture medium. The flasks were inoculated with 1 mL spore suspension of *U. isabellina* CBS 194.28 containing 3×10^7 CFU mL⁻¹, prepared as described in Meeuwse et al. [16], and incubated at 25 °C in a shaking incubator at 225 rpm for 3 days. To avoid transfer of non-consumed C-source or N-source to the main culture, 10–80 mL of pre-culture, depending on the desired initial amount of biomass, was centrifuged (10 min, 4,000g) and resuspended in 40 mL medium without C-source and N-source.

Batch cultures

The batch cultures were carried out in a baffled glass bioreactor at 28 °C with stirring (700 rpm), aeration (1 L min⁻¹), pH-control and off-gas analysis as was described before in Meeuwse et al. [16]. Each batch culture was started by adding 40 mL of pre-culture without C-source or N-source to obtain a final volume of 2 L. Six cultivations were done with different initial amounts of biomass, in order to obtain runs that were out of phase and to reduce nocturnal gaps in sampling. The phase differences were chosen to allow even distribution of sampling in time. Samples were taken every 2 h during daytime. The bioreactor was placed on a balance and the total mass of the bioreactor was logged on-line using labview 5.1 (National Instruments, US). From this mass the liquid volume in the bioreactor was calculated, which was used to correct for changes in culture volume because of sampling, evaporation and addition of NaOH and medium.

All cultures were started at an initial glucose concentration of 100 mM (C/N-ratio 30 Cmol Nmol⁻¹). 200 mL glucose solution (1 M) was added to two out of the six cultures immediately after the exhaustion of the N-source in the medium, leading to a theoretical initial glucose concentration of 200 mM (C/N-ratio 60 Cmol Nmol⁻¹).

Analysis

Samples taken from the reactor were processed and analyzed as described in Meeuwse et al. [16]. The biomass, dry weight, ash content, elemental composition and lipid content were determined as described before [16]. The medium was analyzed for glucose and TOC as described before [16], and the NH₄⁺ concentration was measured

with an ammonium test kit (LCK 303, Hach Lange, Germany).

Results and discussion

Batch culture results

Six batch cultivations were carried out. In all cases the initial glucose concentration was 600 Cmol m⁻³ and the initial NH₄⁺ concentration was 20 Nmol m⁻³ (C/N = 30 Cmol Nmol⁻¹). In two of the six cultures, extra glucose was added immediately after the exhaustion of NH₄⁺; this resulted in a total glucose addition of 1,200 Cmol m⁻³ (C/N = 60 Cmol Nmol⁻¹). The extra glucose was not added at the start of the experiments because preliminary results (not published) showed that a high initial glucose concentration (>1,000 Cmol m⁻³) caused formation of an unknown byproduct. To avoid this, we kept the glucose concentration during exponential growth ≤ 600 Cmol m⁻³.

Each batch culture was inoculated with a different amount of biomass to obtain different lengths of the exponential phase, as is shown by the CO₂-production rate in Fig. 2a. This made it possible to take samples covering the whole time range of the culture equally, without the need for sampling during the night. To facilitate the determination of model parameters from results of all cultures, we shifted the data points from all but one culture in time in such a way that the end of the exponential phase coincided, as is shown in Fig. 2b. Cultures with the same initial C/N-ratios gave very similar CO₂-production rates and therefore it is allowed to combine data points obtained from different cultures.

Figure 3 shows all measured data. All data obtained before the addition of extra glucose are shown in Fig. 3a, b; data obtained after extra glucose addition are shown only in Fig. 3b. Arrows in Fig. 3b indicate the glucose addition. Microscopic examination showed that the biomass was present as loose filaments and very small pellets with an average size of 100–200 μm, which means that exponential growth was possible. Figure 3 shows that the total biomass concentration indeed increased exponentially as long as NH₄⁺ was present, and the lipid fraction remained constant. When NH₄⁺ was exhausted, the lipid fraction started to increase. At the moment of NH₄⁺-exhaustion, both the CO₂-production rate and the O₂-consumption rate suddenly decreased and then increased again. The nitrogen fraction of the cells decreased from 7.6 to 5.7% w/w, while the lipid fraction only increased from 4 to 8% w/w in the same period. Calculations show that the decrease of the nitrogen fraction cannot be explained by lipid production alone; therefore, we assume that a second carbon-based storage product accumulated, which we assume to be

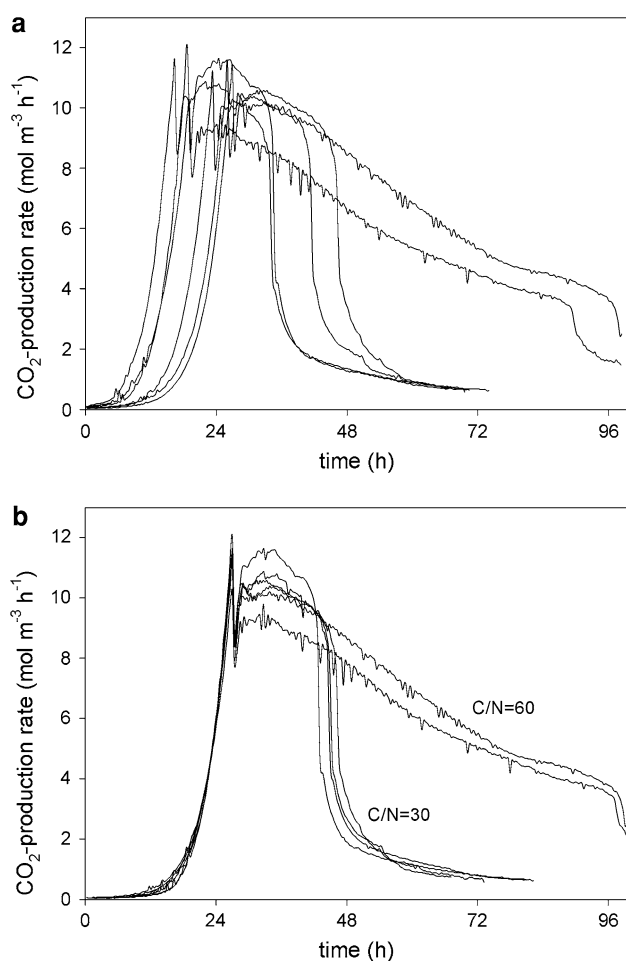


Fig. 2 CO₂-production rate during the six batch cultures **a** as measured in time and **b** after shifting of the time axis of all but one culture to let the end of the exponential phase coincide with each other. Four of the fermentations had an initial C/N-ratio of 30 Cmol Nm⁻¹, while in two fermentations the theoretical initial C/N-ratio was increased to 60 Cmol Nm⁻¹ after the exponential growth phase

carbohydrates. Accumulation of carbohydrates by oleaginous yeast has been described in the literature [20, 21].

Figure 3b shows that the lipid production rate gradually decreased in time; this is also visible in the decreasing respiration rates. The lipid fraction in the cells did not increase significantly anymore after 72 h, while the glucose was not yet exhausted (>5 g L⁻¹). The addition of extra glucose after 72 h did not have any effect on lipid production (results not shown). This shows that the lipid production was not limited by glucose, as was previously described [13, 14]. The maximum lipid fraction reached was around 45% w/w (Fig. 3b), which is lower than lipid fractions reported in literature (55–74% w/w) for batch cultures with a different strain of the same species using glucose as C-source [23, 24].

In Fig. 3a, a linear decrease of the lipid fraction is visible after glucose is exhausted. Because the cells store the

lipids as a reserve material, it is reasonable to assume that they use it as an energy source when the external energy source is exhausted. We assume that the cells use the lipids for maintenance, because growth is not possible in the absence of an N-source. Growth with accumulated lipids as C-source was only observed for cultures with a low initial C/N-ratio [10–12].

Figure 4 compares the carbon-containing products (lipid-free biomass, lipids, CO₂) with the consumed glucose. C-recovery decreased when more than 700 Cmol m⁻³ of glucose was consumed, after approximately 50 h. Measurements of the total carbon content of the medium showed that only a minor part of the missing carbon was present in the medium as unknown product or cell debris (results not shown). We conclude that the major part of the missing carbon was present in the observed biomass aggregates attached to the walls and stirrer of the bioreactor, and was therefore not recovered in the broth samples.

Figure 5 shows the composition of the accumulated lipids for all cultures. During exponential growth (until 27 h), the lipids have an average composition of $30 \pm 1\%$ C16:0, $1.5 \pm 0.2\%$ C16:1, $12 \pm 2\%$ C18:0, $39 \pm 1\%$ C18:1 and $18 \pm 1\%$ C18:2 fatty acids. After the exponential growth phase, the composition changes over a period of approximately 10 h and then remains constant. The constant composition during lipid accumulation and lipid turnover was $25 \pm 1\%$ C16:0, $1.3 \pm 0.1\%$ C16:1, $6 \pm 1\%$ C18:0, $54 \pm 1\%$ C18:1 and $14 \pm 1\%$ C18:2. This is consistent with findings in chemostat experiments with this strain [16] and with results from literature for the same species during the lipid accumulation phase in batch cultures with glucose as C-source [24, 25]. The largest change between the growth phase and the lipid production phase is seen for C18:1. Fakas et al. [26] showed that C18:1 is more abundant in the neutral lipid fraction of the cell (storage lipids) than in the phospholipid fraction (membrane lipids) in the same species, which is consistent with our findings.

Fitting procedure

Ten model parameters (μ_{\max} , $C_X(0)$, f_{L0} , Y_{XN} , $f_{P\max}$, Y_{XS} , Y_{LS} , m_L , $q_{L\max}$, k_d) were determined by fitting the model on the data as explained below. The obtained parameter values are shown in Table 1. The initial biomass concentrations in our cultures were too low to measure accurately. Therefore, we determined values for μ_{\max} and $C_X(0)$ by fitting the equation for exponential growth (Eq. 1) on all data points with NH₄⁺ present. The minimum lipid fraction of the cells, f_{L0} , was calculated from the average lipid fraction of cells during exponential growth. The yield of basic biomass on N-source, Y_{XN} , was determined by linear regression analysis using lipid-free

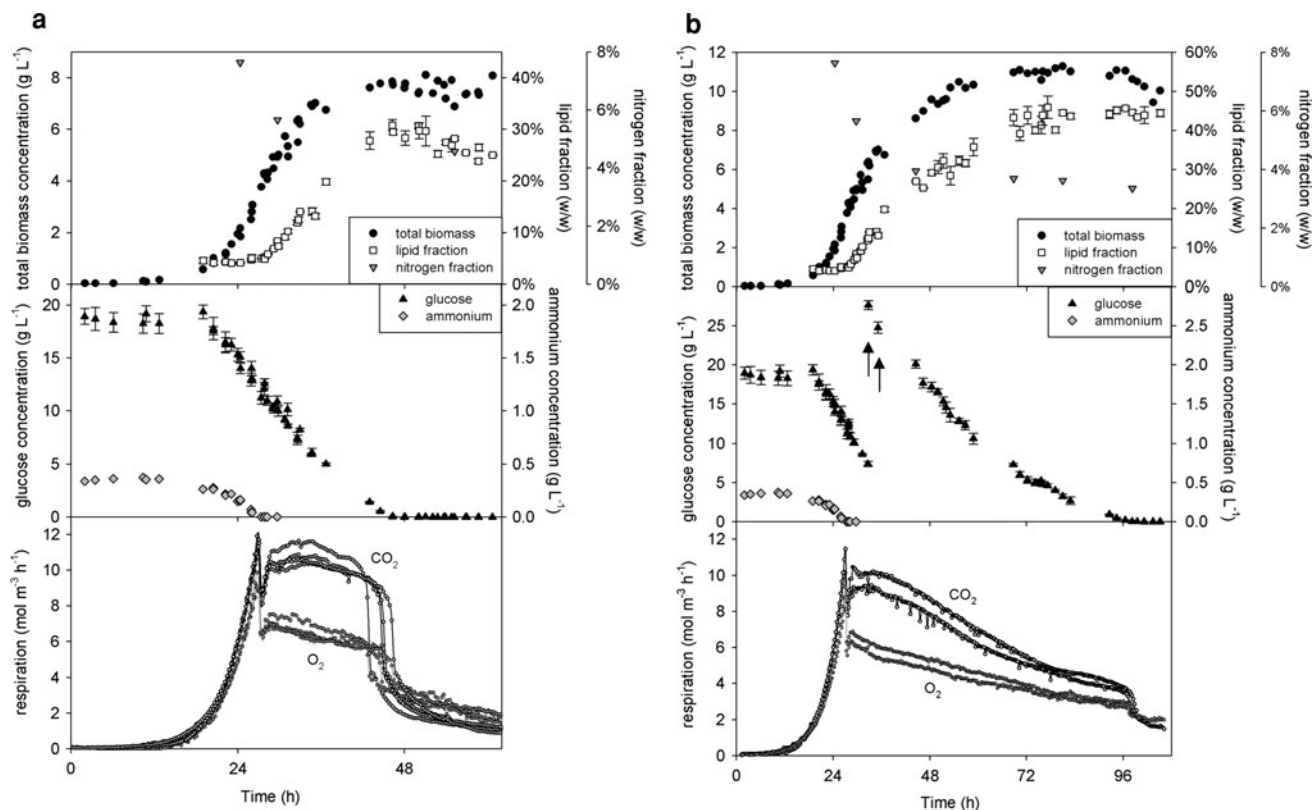


Fig. 3 Results of batch cultures with *U. isabellina* on glucose and NH_4^+ **a** with an initial C/N-ratio of $30 \text{ Cmole Nmol}^{-1}$, **b** with an initial C/N-ratio of $30 \text{ Cmole Nmol}^{-1}$ and addition of extra glucose

(indicated with *arrows*) to a theoretical initial C/N-ratio of $60 \text{ Cmole Nmol}^{-1}$. *Error bars* indicate SD

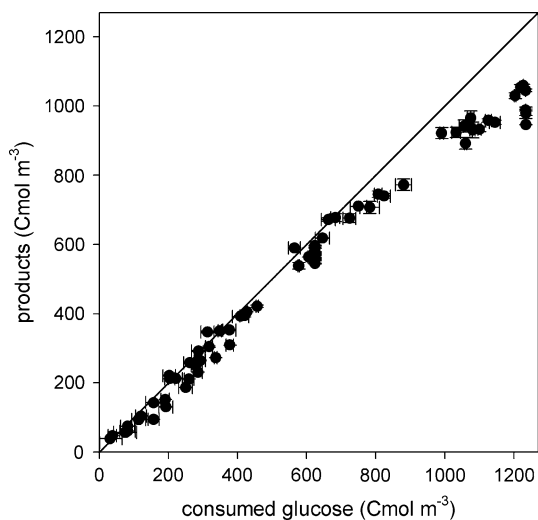


Fig. 4 Carbon recovery as a function of consumed glucose. *Error bars* indicate SD

biomass data and N-source consumption data in Fig. 6a. This figure shows a good correlation ($r^2 = 0.97$) before N-depletion. After N-depletion, the lipid-free biomass

concentration increased, indicating accumulation of a storage compound which we assume to be carbohydrates. The maximum carbohydrate fraction in the cells, f_{Pmax} , was calculated from the average lipid-free biomass concentration for $t > 35 \text{ h}$ divided by the maximum basic biomass concentration (C_{Xmax}) from Eq. 8. We determined the maintenance coefficient, m_L , from the decrease in the lipid fraction after glucose was exhausted, according to Eq. 16. Data from the cultures with C/N = $60 \text{ Cmole Nmol}^{-1}$ were not used. The result of this linear regression analysis is shown in Fig. 6b. The parameters Y_{XS} , Y_{LS} , q_{Lmax} and k_d were determined simultaneously by non-linear regression analysis using all data for the total biomass concentration, the lipid fraction of the cells, the glucose concentration and the CO_2 and O_2 -production rates, i.e. all data shown in Fig. 3 except the nitrogen fraction in the cells. All values were divided by the median value and the number of data points for that variable to give all variables an equal weight in the fitting procedure. For the yield of carbohydrates on C-source, Y_{PS} , we used the theoretical value of $Y_{PS} = 1 \text{ Cmole Cmole}^{-1}$. The two remaining parameters q_P and m_S were calculated from Eqs. 12 and 17, respectively.

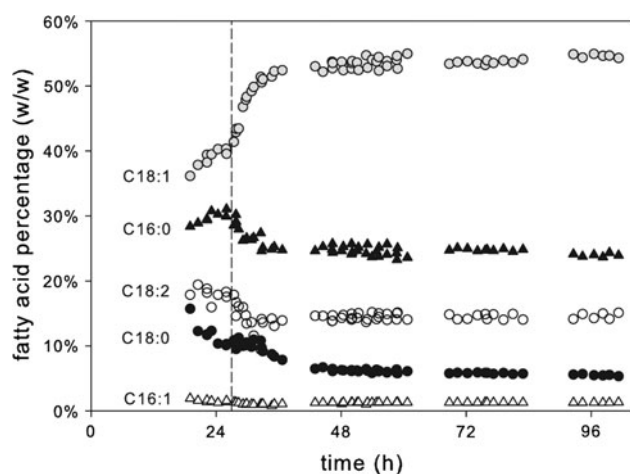


Fig. 5 Composition of the accumulated lipids in the cells in time divided into the five measured fatty acids. The vertical line at 27 h indicates the end of the exponential growth phase and the start of N-source limitation

Fit of the model to the data

Figure 7 compares the measurements and the results of model calculations with the parameter values in Table 1. Vertical lines divide the figures in three periods that are described in the model: growth, lipid accumulation and lipid turnover. The calculated biomass concentration is shown as total biomass, lipid-free biomass (including carbohydrates) and basic biomass. Only the model prediction is shown for the basic biomass concentration (lipid-free, carbohydrate-free biomass), because carbohydrates were not measured. In Fig. 7b, the glucose concentrations before addition of extra glucose were recalculated as if the glucose was added at the start of the culture.

In the exponential growth phase, the model describes all measured variables very well ($r^2 = 0.99$ for lipid-free biomass, basic biomass and CO_2 production rate). The substrate concentrations are predicted accurately by the model. There is no sign of deceleration in the substrate consumption at low concentrations, which shows that the assumed zero-order kinetics can be used.

In the accumulation phase, carbohydrate accumulation and the trend of lipid accumulation are predicted well, but the lipid concentrations and the respiration rates are overestimated later in the experiments, while the measured lipid-free biomass concentration is not as constant as the model predicts. These deviations are caused by the decrease in C-recovery at the end of the cultures with high C/N-ratio (Fig. 4). The model assigns the missing carbon to lipids and CO_2 , which are therefore overestimated. However, the trend predicted by the model agrees with that of the data. For all experiments, the observed decrease in CO_2 production rate (Fig. 7b) from 29 h (directly after the exponential phase) until 97 h (when glucose is exhausted)

could be fitted with exponential functions with constants of -0.016 h^{-1} ($r^2 = 0.99$, $n = 225$ for both experiments). This shows that the decrease in lipid production rate is indeed exponential and that the value for k_d in Table 1 is valid. Furthermore, the observed ratio between the CO_2 production rate and the O_2 consumption rate (RQ) decreases during the lipid production phase from 1.7 to 1.3 mol mol^{-1} (Fig. 7b), while the model predicts a decrease from 1.6 to 1.3 mol mol^{-1} . In our model, we assumed that the lipid accumulation starts immediately with the maximum rate and we neglected the delay in the lipid accumulation that is visible in the respiration measurements. Boulton and Ratledge [20] described the transition from carbon-limited to nitrogen-limited conditions for the oleaginous yeast *Lipomyces starkeyi*; they found that it takes several hours for the culture to adapt to the new situation. Figure 7 shows that the overall fit of the model on the data is hardly influenced by our assumption.

Figure 7a shows a clear decrease of lipids in the turnover phase and no increase of basic biomass during this phase. The lipid turnover rate is predicted very well, even though the lipid concentration is slightly overestimated due to the over-prediction in the accumulation phase explained in the previous section. The respiration rate during the third phase is also overestimated; but the predicted RQ is correct: 0.7 mol mol^{-1} . This means that lipid turnover is taking place as predicted.

We conclude that the model describes the physiology and kinetics of the lipid-accumulating fungus *U. isabellina* in batch cultures quite well. The model reveals that the low total mass yield of lipids on glucose reached (14% w/w for both cultures) is partially caused by the ‘wasting’ of glucose for carbohydrates (up to 20% of consumed glucose) and maintenance (up to 19% of consumed glucose). Carbohydrate storage is not a problem exclusively for the strain we used; it has been measured before [20, 21], and we found evidence for carbohydrate storage in other cultures from the literature [17]. It could be debated whether the stored component in our cultures was indeed a carbohydrate; fungi are also known to accumulate, for example polyols [28]. However, polyol quantities in fungi are generally small as compared to glycogen and trehalose quantities [18, 19]. Furthermore, Fig. 7 shows that the degree of reduction of the storage product (4 Cmol^{-1}) used in the calculations gives a good fit of the respiration rates. Polyols have a higher degree of reduction, which would lead to a lower O_2 consumption rate. Therefore, we believe that the assumption that the cells accumulate carbohydrates is reasonable.

Finally, the model shows how rapidly the lipids are lost due to maintenance when the external C-source is depleted. In a well-mixed batch culture, lipid turnover can be avoided by harvesting the cells at the right moment. Lipid

Table 1 Parameter values used to fit our data set, and parameter values for a chemostat culture [16] and another batch culture [14] from literature, with the parameter values given in the source article, and found by fitting our model on this data set

Parameter	Symbol	Batch ($n = 80$) (this study)	Chemostat ($n = 12$) [16]	Batch on sweet sorghum [14], values from literature	Batch on sweet sorghum [14], values from this study (Fig. 8)
Yield of lipid-free biomass on NH_4^+	Y_{XN} (Cmol Nmol ⁻¹)	5.5 ± 0.2	6.1 ± 0.7	8.9–11.1 ^a	6.1 ± 0.2
Yield of lipid-free biomass on glucose	Y_{XS} (Cmol Cmol ⁻¹)	0.78 ± 0.01	0.92 ± 0.10	0.21–0.36 ^a	0.51 ± 0.03^b
Yield of lipids on glucose	Y_{LS} (Cmol Cmol ⁻¹)	0.56 ± 0.01	(0.59) ^c	0.27–0.46 ^a	0.39 ± 0.01
Yield of carbohydrates on glucose	Y_{PS} (Cmol Cmol ⁻¹)	1 ^d	–	–	1 ^d
Maintenance on lipids	m_{L} (Cmol Cmol ⁻¹ h ⁻¹)	0.020 ± 0.004	–	–	0 ^e
Maintenance on glucose	m_{S} (Cmol Cmol ⁻¹ h ⁻¹)	0.028 ± 0.006	0.05 ± 0.01	–	0 ^e
Minimum lipid fraction	f_{LO} [Cmol lipids (Cmol total biomass) ⁻¹]	0.078 ± 0.006	0.079	–	0.08 ^f
Maximum carbohydrate fraction	f_{Pmax} [Cmol carbohydrates (Cmol basic biomass) ⁻¹]	0.87 ± 0.17	–	–	ND ^g
Maximum specific growth rate	μ_{max} (h ⁻¹)	0.21 ± 0.01	0.23 ± 0.02	0.566 (<0.23) ^h	0.26 ± 0.01
Maximum specific lipid production rate	q_{Lmax} (Cmol Cmol ⁻¹ h ⁻¹)	$0.090 \pm 0.003e^{-k_{\text{at}}}$	0.023 ± 0.006	0.785 (<0.038) ⁱ	$0.083 \pm 0.003e^{-k_{\text{at}}}$
Time constant decrease lipid production rate	k_{d} (h ⁻¹)	0.016 ± 0.001	–	–	0.028 ± 0.001
Maximum carbohydrate accumulation rate	q_{P} (Cmol Cmol ⁻¹ h ⁻¹)	0.14 ± 0.01	–	–	0.006 ± 0.001
Initial biomass concentration	$C_{\text{X}}(0)$ (Cmol m ⁻³)	0.36 ± 0.09	NA	Multiple	Multiple

All values are mean \pm SD

^a Both an experimental value as well as a fitted value are given

^b We assumed that only 95% of the sugars could be consumed

^c Theoretical value [27]

^d Theoretical value

^e No significant value above zero was found

^f Estimated to be 5% w/w because lipid measurements at low biomass concentrations were not accurate enough to fit a value

^g Assumed not to be reached in the experiments

^h Number in parenthesis is the maximum specific growth rate possible at the initial substrate concentrations in our cultures as well as the sweet sorghum cultures used according to the used Andrews' equation for double substrate limitation and C-source inhibition

ⁱ Number in parenthesis is the maximum value possible according to the used Andrews' equation for double substrate limitation and C-source inhibition

turnover might be a problem in inhomogeneous cultures where local depletion of C-source can occur before the average concentration is zero. Repression of lipid turnover by multiple limitations as described by Papanikolaou et al. [29] might be an option to circumvent this, if this is feasible with the used (solid) substrate.

Lipid production mechanisms

Table 1 compares values found in batch cultures and chemostat cultures with *U. isabellina* [16]. Most of the

parameter values are similar, but there are some exceptions. The values found for the yield of basic biomass on glucose (Y_{XS}) and for the maintenance coefficient (m_{S}) in batch are lower than in chemostat. However, they are also more accurate because they are based solely on data from the exponential growth phase where the carbon recovery was complete, while in the chemostat cultures the carbon recovery was incomplete.

There is also a striking difference between the maximum specific lipid production rate, q_{Lmax} , found in batch and chemostat cultures. The initial specific lipid production rate

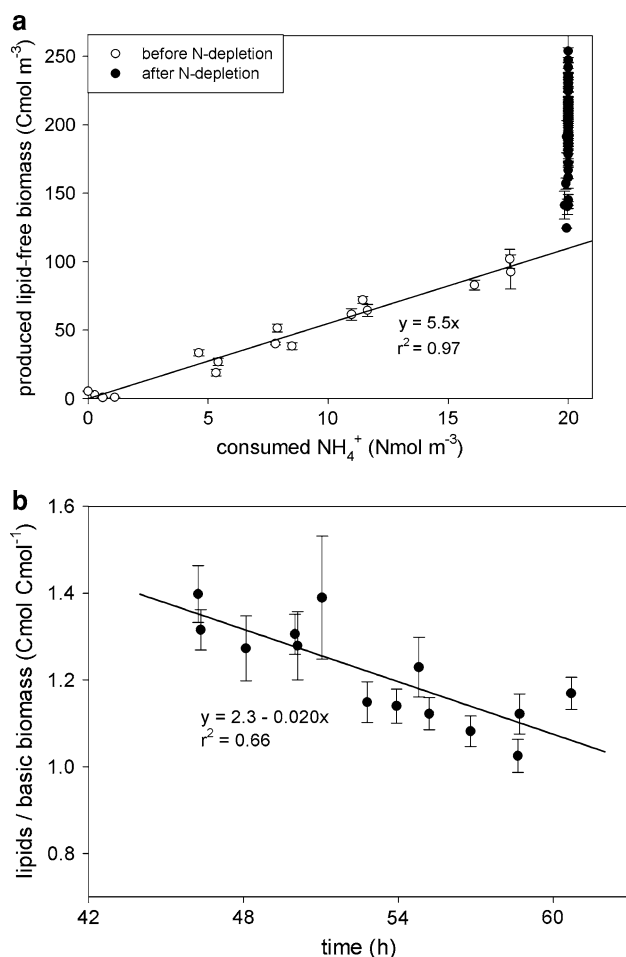


Fig. 6 Graphs for parameter value determination. Error bars indicate SD. **a** Lipid-free biomass including carbohydrates versus N-consumption for linear regression analysis. The slope of the curve is equal to the yield of basic biomass on N-source Y_{XN} . The increase of lipid-free biomass without extra N-consumption is assumed to be caused by carbohydrate accumulation. **b** The lipid concentration divided by the basic biomass concentration versus the time during lipid turnover (initial substrate ratio: $C/N = 30 \text{ Cmol Nmol}^{-1}$)

in batch cultures is almost four times higher than the constant value found in chemostat cultures [16]. Furthermore, q_{Lmax} in chemostat cultures was independent of the residence time (=cell age), while there was an exponential decrease in batch cultures. The value of q_{Lmax} in chemostat cultures is very close to the specific functional lipid production rate, i.e. the production rate needed to obtain a lipid fraction f_{L0} in cells growing at μ_{max} [17]. This suggests that the fungus uses the enzymes that normally produce functional or membrane lipids to accumulate lipids in chemostat cultures. The much higher initial specific lipid production rate in batch cultures, which decreases in time according to a first order decay mode, might indicate that another mechanism is used.

Ratledge and Wynn [30] proposed that lipid accumulation in batch cultures is caused by continuation of glucose

assimilation while growth slows down or stops because of nitrogen limitation. In our model, we assume that the specific glucose uptake rate after N-source depletion remains equal to the specific uptake rate during exponential growth. This gives an accurate prediction and therefore supports the proposition of Ratledge and Wynn [30]. However, part of the glucose taken up by the cell is accumulated as carbohydrates instead of being converted to citric acid and subsequently to lipids. The reason for the carbohydrate accumulation could be a kinetic bottleneck in the conversion of citric acid to fatty acids; it cannot be the conversion of glucose to citric acid or the respiration as these processes had a higher rate during exponential growth.

Wynn et al. [9, 15] described a switch from normal growth to lipid accumulation in batch cultures of *Mucor circinelloides* and *Mortierella alpina* when they encounter nitrogen limitation; a decrease in intracellular NH_4^+ inhibits the activity of the enzyme phosphofructokinase, leading to accumulation of citrate, which is the source of acetyl-CoA used for lipid production [9]. Wynn et al. [15] also reported a decrease in lipid production rate in time, which could be attributed to a decrease in activity of malic enzyme, the rate-limiting enzyme in the lipid production route. Their limited number of data points [15] suggests that the observed decrease in enzyme activity is exponential, as we found in our cultures. The decrease is irreversible because malic enzyme activity can only be restored by de novo synthesis [15], which requires an N-source. Although we have no enzyme activity data, it seems likely that the decrease in specific lipid production rate in our batch reactors was caused by degradation of malic enzyme, which could not be synthesized because of the lack of N-source. In chemostat culture, the continuous supply of N-source would allow continuous protein synthesis, which could explain the observed constant value of the maximum specific lipid production rate [16].

Comparison to literature

Table 1 compares our parameter values to values reported by Economou et al. [14] for batch cultures of a different strain of the same species with sweet sorghum extract as substrate. In addition, we fitted our model on the same data; parameter values found are also shown in Table 1 and the resulting fit is shown in Fig. 8. This graph shows that our model fits the experimental data well, although the underestimation of the lipid production rate in Fig. 8a could indicate that substrate inhibition was important in Fig. 8b, c, which was not included in our model. However, the sum of squares of residuals for all fitted data points (for lipid-free biomass, lipids and sugars in the three presented graphs) was three times lower than for the original model developed

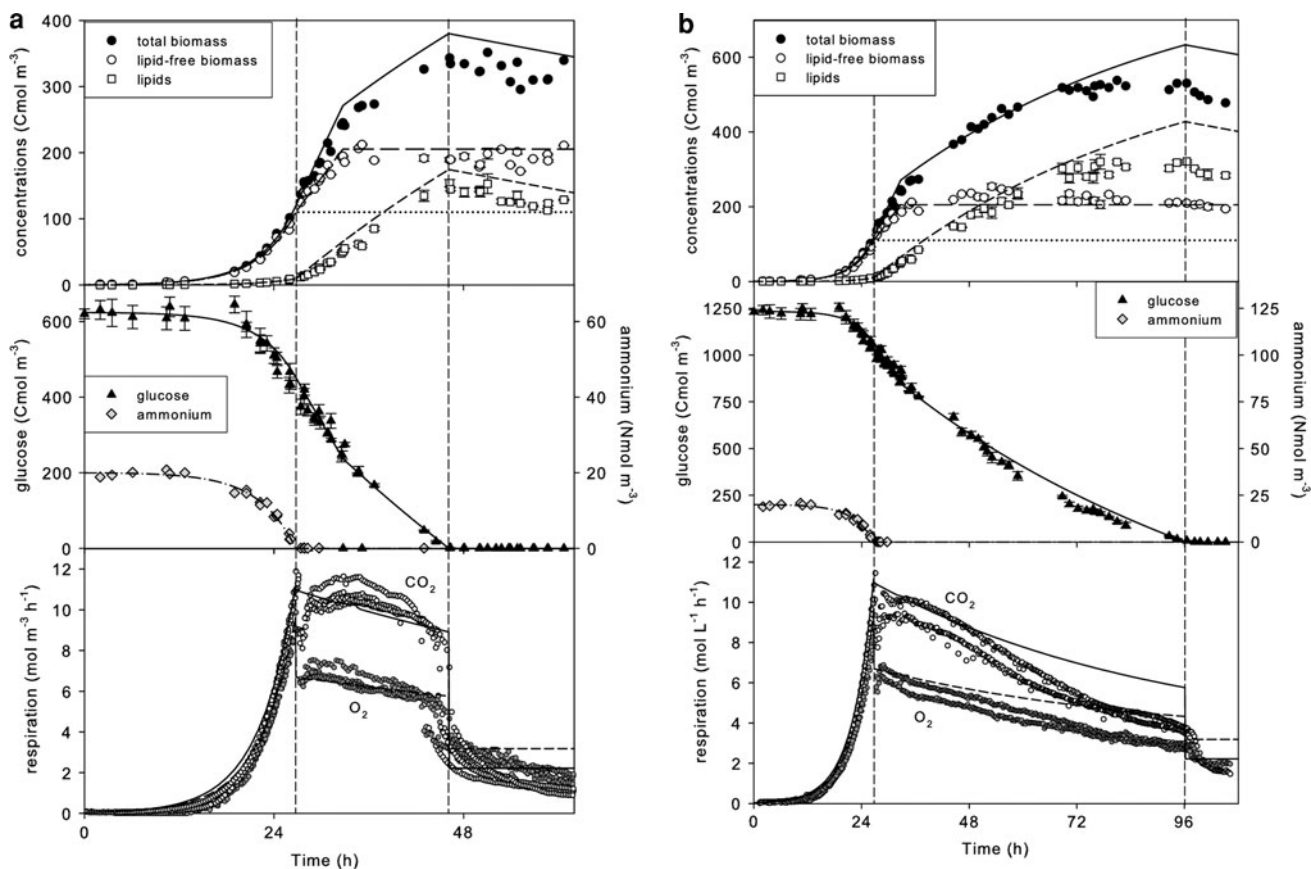


Fig. 7 Fit of the model on the results of batch cultures with *U. isabellina* on glucose and NH_4^+ **a** with an initial C/N-ratio of $30 \text{ Cmol Nmol}^{-1}$, **b** with a (theoretical) initial C/N-ratio of

$60 \text{ Cmol Nmol}^{-1}$. Error bars indicate SD. Vertical lines divide the graphs in three phases in time: the growth phase, the lipid accumulation phase and the lipid turnover phase

for these data points [14]. We also fitted our model successfully on published results [7, 8] of batch cultures of the oleaginous yeast *Rhodotorula gracilis* (results not shown). This shows that our model is suitable for other data sets with different C/N-ratios, strains and substrates.

Table 1 shows that there are some significant differences between the parameter values for the different models and data sets. Both μ_{\max} and $q_{L\max}$ determined by Economou et al. [14] are much higher than our values for both data sets because they used Monod kinetics and substrate inhibition in their model, which leads to very high maximum values. The actual specific rates shown in Table 1 are similar to our values. The yield values Y_{XS} and Y_{LS} are lower for the sweet sorghum batches, both the values from literature and our values; this may have been caused by differences in substrate or strain. The value for Y_{XN} obtained by Economou et al. [14] is higher and close to the yield of lipid-free biomass including carbohydrates in our experiments ($10.5 \text{ Cmol Nmol}^{-1}$). This may indicate that carbohydrates were produced in their cultures, which is also supported by the observed production of

lipid-free biomass after N-depletion [14]. We therefore included carbohydrate production in our fit, which results in a value for Y_{XN} similar to the value from our experiments, combined with a very low specific carbohydrate production rate (Table 1). This rate could not be described by Eq. 12; we used a constant fitted value instead, which leads to a good fit.

The most important parameter for lipid accumulation is $q_{L\max}$. Therefore, we compared our value to literature values from other batch cultures; the large difference in $q_{L\max}$ for batch and chemostat cultures shown in the previous paragraph means that comparison to values from chemostats is not useful. Our value for $q_{L\max}$ is high compared to the values found for *R. gracilis* on glucose ($0.025 \text{ Cmol Cmol}^{-1} \text{ h}^{-1}$) [6] and *C. curvata* on whey ($0.040 \text{ Cmol Cmol}^{-1} \text{ h}^{-1}$) [13]. However, all values are of the same order of magnitude and therefore our value is reasonable. Our $q_{L\max}$ value is lower than values found for batch cultures using lipid-based substrates ($0.09\text{--}0.25 \text{ Cmol Cmol}^{-1} \text{ h}^{-1}$) [11, 12], which is not surprising because less transformations are needed when lipids are used as starting material for lipid accumulation.

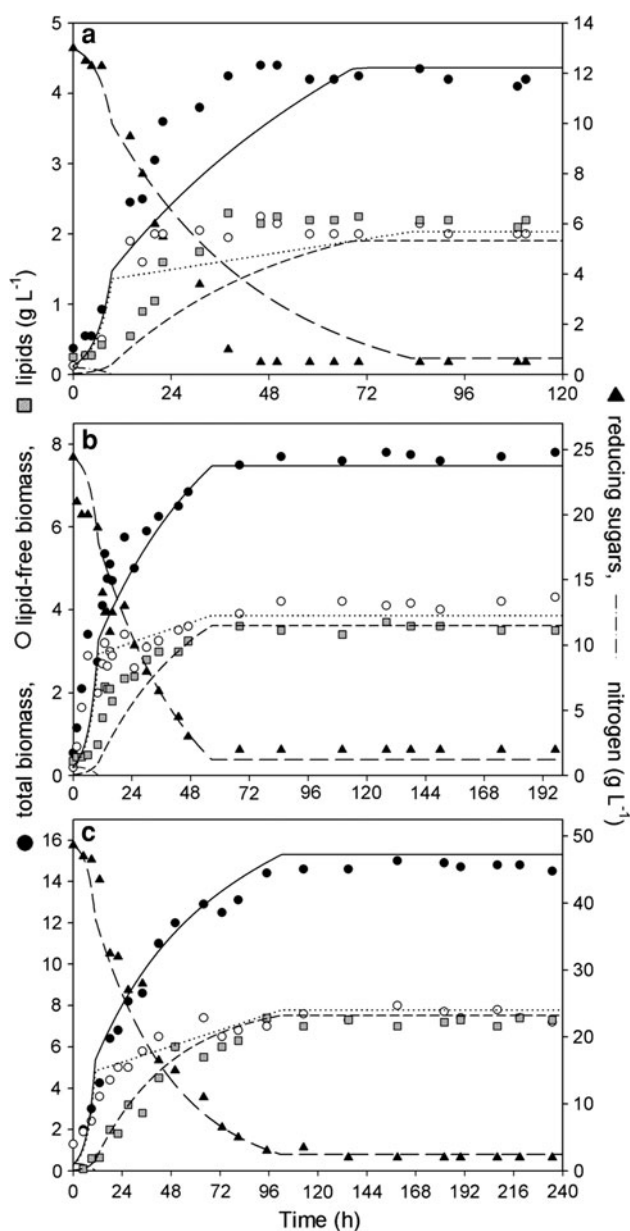


Fig. 8 Fit of our model to batch culture data of *M. isabellina* on sweet sorghum extract from Economou et al. [14], Fig. 1. Used parameter values are shown in Table 1. We assumed that 5% of the sugars could not be consumed

Conclusions

We developed a model for submerged batch culture of oleaginous fungi and validated it with data from batch cultures of *U. isabellina* growing on glucose and NH_4^+ . The deviation between model and data was small and could be explained by incomplete carbon recovery near the end of the cultures, due to aggregation of cells on baffles and stirrer. The model shows that a batch culture can be divided into three phases: the growth phase, the lipid accumulation phase and the lipid turnover phase. In the first phase, no

substrate is limiting and growth occurs at the maximum specific growth rate, while only a basic lipid fraction for functional lipids is present in the cells. When the nitrogen source is exhausted, the cells accumulate carbohydrates up to a maximum fraction, and lipids with an exponentially decreasing specific rate. We showed that this decrease was not caused by the declining C-source concentration, and therefore could not be described with Monod kinetics, as was done in other models for submerged batch culture [13, 14]. The specific rate of lipid production in batch cultures is much higher than in chemostat cultures, indicating that another lipid synthesis mechanism is active. Observations during the lipid production phase and results from the literature [9, 16, 20] indicate that in batch cultures a switch from growth to lipid accumulation takes place, while in chemostat cultures growth and lipid production occur simultaneously, which leads to different rates. When the C-source is exhausted, lipids are combusted for maintenance requirements, and not for growth as described before [14].

The model developed in this paper described all observed features of a submerged batch culture well, including turnover of lipids for maintenance and the decrease in lipid production rate that was observed to be independent of the C-source concentration. It also describes results from literature well. Therefore, it is a useful addition to previously published models [5–8, 10–14].

Acknowledgments This work was financially supported by the DEN program of SenterNovem under project number 2020-03-12-14-006. The authors would like to thank Sebastiaan Haemers and Fred van den End for their technical support.

Open Access This article is distributed under the terms of the Creative Commons Attribution Noncommercial License which permits any noncommercial use, distribution, and reproduction in any medium, provided the original author(s) and source are credited.

References

1. Certik M, Shimizu S (1999) Production and application of single cell oils. *Agro Food Ind Hi-Tech* 10:26–32
2. Li Q, Du W, Liu DH (2008) Perspectives of microbial oils for biodiesel production. *Appl Microbiol Biotechnol* 80:749–756
3. Meng X, Yang JM, Xu X, Zhang L, Nie QJ, Xian M (2009) Biodiesel production from oleaginous microorganisms. *Renew Energy* 34:1–5
4. Feofilova EP, Sergeeva YE, Ivashechkin AA (2009) Biodiesel-fuel: content, production, producers, contemporary biotechnology (Review). *Appl Biochem Microbiol* 46:369–378
5. Granger LM, Perlot P, Goma G, Pareilleux A (1993) Efficiency of fatty acid synthesis by oleaginous yeasts—prediction of yield and fatty acid cell content from consumed C/N ratio by a simple method. *Biotechnol Bioeng* 42:1151–1156
6. Sattur AP, Karanth NG (1989) Production of microbial lipids. I. Development of a mathematical model. *Biotechnol Bioeng* 34:863–867

7. Sattur AP, Karanth NG (1991) Mathematical modeling of production of microbial lipids. 1. Kinetics of biomass growth. *Bioprocess Eng* 6:227–234
8. Karanth NG, Sattur AP (1991) Mathematical modeling of production microbial lipids. 2. Kinetics of lipid accumulation. *Bioprocess Eng* 6:241–248
9. Wynn JP, Hamid AA, Li YH, Ratledge C (2001) Biochemical events leading to the diversion of carbon into storage lipids in the oleaginous fungi *Mucor circinelloides* and *Mortierella alpina*. *Microbiology* 147:2857–2864
10. Aggelis G, Komaitis M, Papanikolaou S, Papadopoulos G (1995) A mathematical model for the study of lipid accumulation in oleaginous microorganisms. 1. Lipid accumulation during growth of *Mucor circinelloides* Cbs-172–27 on a vegetable oil. *Grasas Aceites* 46:169–173
11. Aggelis G, Sourdis J (1997) Prediction of lipid accumulation-degradation in oleaginous micro-organisms growing on vegetable oils. *Antonie Van Leeuwenhoek* 72:159–165
12. Papanikolaou S, Aggelis G (2003) Modeling lipid accumulation and degradation in *Yarrowia lipolytica* cultivated on industrial fats. *Curr Microbiol* 46:398–402
13. Glatz BA, Hammond EG, Hsu KH, Baehman L, Bati N, Bednarski W, Brown D, Floetenmeyer M (1984) Production and modification of fats and oils by yeast fermentation. In: Ratledge C, Dawson PSS, Rattray J (eds) *Biotechnology for the oils and fats industry*. American Oil Chemists' Society, Urbana, pp 163–176
14. Economou CN, Aggelis G, Pavlou S, Vayenas DV (2011) Modeling of single-cell oil production under nitrogen-limited and substrate inhibition conditions. *Biotechnol Bioeng* 108:1049–1055
15. Wynn JP, Hamid ABA, Ratledge C (1999) The role of malic enzyme in the regulation of lipid accumulation in filamentous fungi. *Microbiology* 145:1911–1917
16. Meeuwse P, Tramper J, Rinzema A (2011) Modeling lipid accumulation in oleaginous fungi in chemostat cultures. I. Development and validation of a chemostat model for *Umbelopsis isabellina*. *Bioprocess Biosyst Eng* 34:939–949
17. Meeuwse P, Tramper J, Rinzema A (2011) Modeling lipid accumulation in oleaginous fungi in chemostat cultures. II. Validation of the chemostat model using yeast culture data from literature. *Bioprocess Biosyst Eng* 34:951–961
18. Griffin DH (1993) *Fungal physiology*, 2nd edn. Wiley, New York
19. Gow NAR, Gadd GM (1995) *The growing fungus*. Chapman & Hall, London
20. Boulton CA, Ratledge C (1983) Use of transition studies in continuous cultures of *Lipomyces starkeyi*, an oleaginous yeast, to investigate the physiology of lipid accumulation. *J Gen Microbiol* 129:2871–2876
21. Ykema A, Verbree EC, Vanverseveld HW, Smit H (1986) Mathematical modeling of lipid production by oleaginous yeasts in continuous cultures. *Antonie Van Leeuwenhoek* 52:491–506
22. Vishniac W, Santer M (1957) Thiobacilli. *Bacteriol Rev* 21:195–213
23. Papanikolaou S, Komaitis M, Aggelis G (2004) Single cell oil (SCO) production by *Mortierella isabellina* grown on high-sugar content media. *Bioresour Technol* 95:287–291
24. Chatzifragkou A, Fakas S, Galiotou-Panayotou M, Komaitis M, Aggelis G, Papanikolaou S (2010) Commercial sugars as substrates for lipid accumulation in *Cunninghamella echinulata* and *Mortierella isabellina* fungi. *Eur J Lipid Sci Technol* 112:1048–1057
25. Papanikolaou S, Galiotou-Panayotou M, Fakas S, Komaitis M, Aggelis G (2007) Lipid production by oleaginous *Mucorales* cultivated on renewable carbon sources. *Eur J Lipid Sci Technol* 109:1060–1070
26. Fakas S, Makri A, Mavromati M, Tselepi M, Aggelis G (2009) Fatty acid composition in lipid fractions lengthwise the mycelium of *Mortierella isabellina* and lipid production by solid state fermentation. *Bioresour Technol* 100:6118–6120
27. Ratledge C (1988) Biochemistry, stoichiometry, substrates and economics. In: Moreton RS (ed) *Single cell oil*. Longman Scientific & Technical, London, pp 33–70
28. Ruijter GJG, Visser J, Rinzema A (2004) Polyol accumulation by *Aspergillus oryzae* at low water activity in solid-state fermentation. *Microbiology* 150:1095–1101
29. Papanikolaou S, Sarantou S, Komaitis M, Aggelis G (2004) Repression of reserve lipid turnover in *Cunninghamella echinulata* and *Mortierella isabellina* cultivated in multiple-limited media. *J Appl Microbiol* 97:867–875
30. Ratledge C, Wynn JP (2002) The biochemistry and molecular biology of lipid accumulation in oleaginous microorganisms. *Adv Appl Microbiol* 51:1–51